Review of Noise Sources in Magnetic Tunnel Junction Sensors

Z. Q. Lei[1], G. J. Li[1], William F. Egelhoff, Jr.[2], P. T. Lai[1], and Philip W. T. Pong[1]

[1]Department of Electrical and Electronic Engineering,The University of Hong Kong, Pokfulam Road, Hong Kong
[2]National Institute of Standards and Technology, Gaithersburg, MD 20899-8552 USA

Noise problem limits the sensitivity of magnetic tunnel junction (MTJ) sensors for ultra-low magnetic field applications. Noise analysis not only helps in finding ways to eliminate noise disturbances but also essential for understanding the electronic and magnetic properties of MTJs. These approaches provide insight for optimizing the design of MTJ sensors before fabrication. This paper reviews the noise sources in MTJ sensors reported in recent years. Both the origins and mathematical derivations of the noise sources are presented, illustrating how different factors affecting the performance of MTJ sensors. A brief outlook of challenges in the future is also given.

Index Terms—**Johnson noise, magnetic noise, magnetic tunnel junction (MTJ), shot noise, thermal noise, $1/f$ noise.**

I. Introduction

A. Magnetic Tunnel Junctions (MTJs) and MTJ Sensors

MAGNETIC TUNNEL JUNCTIONS (MTJs) consist of two ferromagnetic (FM) electrodes separated by an oxide tunnel barrier. MTJs have drawn tremendous attentions for their applications for magnetic field sensors and information storages due to low cost, high sensitivity and large tunneling magnetoresistance (TMR) ratios [1]. TMR can be defined by Julliere's spin-polarized tunneling model [2], $\mathrm{TMR} = 2\mathrm{P}_1\mathrm{P}_2/(1 - \mathrm{P}_1\mathrm{P}_2)$, where P_1 and P_2 are the spin polarizations of current in the electrodes. Theoretical prediction as high as 1000% TMR was derived from wave function matching [3], [4] and 604% TMR was experimentally demonstrated with MgO as the tunnel barrier in MTJs [5]. MTJ sensors are regarded as a competitive candidate in ultra-low field detection, such as biochips and biosensors [6], [7], current imaging on integrated circuits [8], biomedical imaging such as magnetocardiography [9] and magnetoencephalography [10], and weapon detections [11]. MTJ sensors with a detectivity of 2 $\mathrm{pT/Hz}^{1/2}$ at 500 kHz were experimentally achieved by Chave *et al.* [12] and 1 $\mathrm{pT/Hz}^{1/2}$ at 10 kHz was theoretically predicted by Egelhoff *et al.* [13]. Nevertheless, the inevitable noise problem, especially at room temperature and in biomedical detection, is one of the main obstacles for their further applications.

B. Noise Limitations in MTJs

The research focus on MTJs has been mainly on increasing TMR. On one hand, enhancement in TMR can improve the sensitivity of MTJ sensors. On the other hand, the intrinsic noises in MTJs strongly deteriorate the measurement sensitivity and they are limiting the signal-to-noise ratio (SNR). The noises in MTJs need to be eliminated in order to enhance the SNR. Therefore, theoretical and experimental analyses of noises in MTJs are critical for optimizing the performance of MTJ sensors.

C. Purpose of This Review

Although noises limit the SNR of MTJ sensors, their spectra can also be a tool for obtaining intrinsic information of spin-dependent tunneling such as electron transport properties, thermal and magnetic fluctuations. Therefore, a great amount of research efforts were carried out on noise measurements and exploring the origins of noise sources in MTJs. However, there lacks a comprehensive review which systematically review and analyze the mechanisms and mathematical approaches of various noise sources in MTJ sensors reported in the literature. The motivation of this paper is to categorize and summarize the scattered research results and findings on MTJ noises, and to envision feasible methods to reduce MTJ noise floor. In this paper, we review each of the MTJ noise sources. In Section II, the origins of different noise sources in MTJ sensors are specified. In Section III, theoretical modeling of MTJ noises is presented to explain how individual parameter contributes to the noise levels. In Section IV, the approaches for eliminating the noises are discussed based on the analysis results of previous sections. Finally, conclusion and future challenges are included in Section V.

II. Noise Sources in MTJs

Noises in MTJ sensors come from different mechanisms including amplifier noise, thermal electronic noise, shot noise, electronic $1/f$ noise, thermal magnetic noise, magnetic $1/f$ noise, and random telegraph noise (RTN). These noise sources were intensively studied in the past decades and the research results illustrated that all these noise sources in MTJs are incoherent and the total noise can be recognized as the summation or superposition of each noise component [14]–[16]. In this section, background information of these noise sources in MTJs and their origins are discussed.

A. Amplifier Noise

Amplifier noise is not originated from a MTJ junction itself but from the external circuit of the sensor system. An amplifier is needed to increase the amplitude of sensor output signal. Nevertheless, the internal noise from the amplifier deteriorates the sensitivity of the sensor system. Therefore, the amplifier noise

Manuscript received September 15, 2010; revised November 30, 2010; accepted December 12, 2010. Date of current version March 02, 2011. Corresponding author: P. W. T. Pong (e-mail: ppong@eee.hku.hk).

Color versions of one or more of the figures in this paper are available online at http://ieeexplore.ieee.org.

Digital Object Identifier 10.1109/TMAG.2010.2100814

must be characterized and a low-noise amplifier must be used to meet the low-noise requirements for MTJ sensors.

B. Thermal Electronic Noise

Thermal electronic noise is commonly known as thermal noise. The term of thermal electronic noise is used for differentiating from the thermal magnetic noise which is another kind of thermally inspired noise and it is further discussed in later section. Thermal electronic noise is also known as Johnson-Nyquist noise. Johnson and Nyquist first reported in 1928 that the stochastic fluctuation of electric charges exist in all conductors and such thermal agitated electromotive force can be calculated by thermodynamics and statistical mechanics [17], [18]. Thermal electronic noise pervasively appears in all types of conducting media due to the random motions of charge carriers agitated by local temperature variations near Fermi level. These variations provide energy gradient for electrons to overcome the barriers in conducting media. Such an electron migration phenomenon can be regarded as Brownian motion. In MTJs, this thermally induced noise is approximately white noise and it appears in both high- and low-frequency regimes.

C. Shot Noise

Shot noise was discovered in vacuum tubes by Walter Schottky in 1918 [19]. His study demonstrated that there exists a kind of noise even if all the extrinsic noise sources were eliminated. This time-dependent fluctuation phenomenon is associated with the discreteness of electrical charge caused by thermal effects and the stochastic nature of the electron emission process. Since the emission events are uncorrelated, the emission process of an individual electron from cathode can be considered as Poisson distribution. The corresponding fluctuations power density is described by

$$S_I^{shot} = 2eI = S_{Poisson} \tag{1}$$

where e is the electron charge and I is the average dc current of discrete pulses. The factor of 2 appears due to the identical contribution of both positive and negative frequencies [20].

While the Poissonian shot noise is expected in tunneling systems, several research groups [21]–[26] pointed out that the spectrum density of shot noise actually do not always equal to the value calculated by (1) in MTJs (see Fig. 1). Fano factor (F) is used to characterize shot noise [27]. F is defined as the ratio of the actual measured shot noise and the Poissonian value calculated by (1) in an independent electron system, given by the following equation:

$$F = S_{Poisson}/2eI. \tag{2}$$

F is employed to evaluate the correlation with full shot noise $(F = 1)$, whether enhanced $(F > 1)$ or suppressed $(F < 1)$. If the emitting electrons are coherent, F does not equal to 1, and shot noise may not obey Poisson distribution.

As shown in Fig. 1, most of the values of F were found smaller than 1, which means the shot noise undergoes a suppression process due to the correlated electrons in MTJs. In ballistic conductors, (1) represents Poissonian shot noise that the emission of electrons is random and the Coulomb interactions are ignored. However, in mesoscopic MTJ devices, the junction

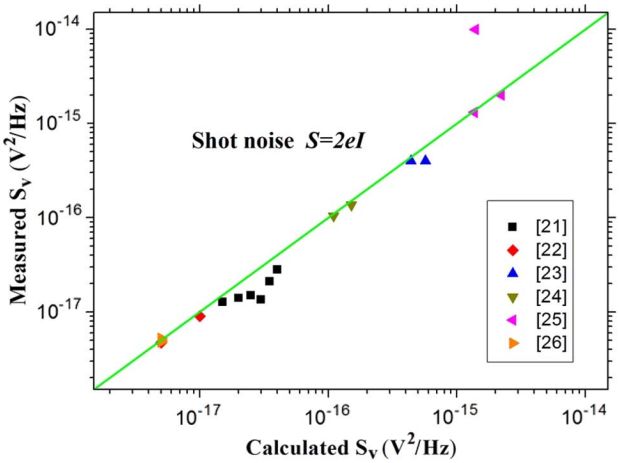

Reference	Barrier	Temperature (K)	F
[21]	Al_2O_3	10	0.45~0.95
[22]	Al_2O_3	10	~1.00
[23]	Al_2O_3	2	0.65
[23]	Al_2O_3	2	~1.00
[24]	Al_2O_3(Cr-doped)	300	~1.00
[25]	Al_2O_3	8	0.90~7.00
[26]	MgO	3.3~12	0.98~1.00

Fig. 1. A plot of calculated shot noise power by equation (1) against measured shot noise power. The data are obtained from the literature listed in the table below the graph. The diagonal line indicates the full shot noise where $F = 1$.

size is small enough for the electrons to become correlated in high biased level, resulting in a sequential tunneling of electrons through the barrier mediated with impurities and a sub-Poissonian shot noise [23]. In sub-Poissonian statistics, electrons are correlated because of the combined action of Coulomb repulsion effect and Pauli exclusion principle. The interactions of Coulomb and Pauli effects limit the density of electrons in real space and phase space respectively. In contrast, a super-Poissonian behavior appears across the barrier in low biased circumstances and enhances the value of F. This is consistent with the enhancement of shot noise phenomenon reported by Garzon *et al.* [25] where the peak value of F is close to 7. The increase of F can be attributed to the combination of spin and charge blockade in the spin-dependent tunneling process.

D. Thermal Magnetic Noise

As the sizes of MTJ junctions keep on shrinking, thermally activated magnetization fluctuations in MTJs become dominating. Thermal magnetic noise is field dependent which is different from the above-mentioned magnetic-independent white noise. Although the origin of thermal magnetic noise is still under investigation, most studies show that it results from the rotations of magnetization in the small volume of a free layer [28]–[30]. Hardner *et al.* [28] found the existence of certain noise at near zero field related to the defects in the antiferromagnetic order in Co/Cu multilayers. The largest noise appeared when the value of dR/dH (the slope of resistance versus field curve) is large and it can be predicted by the fluctuation-dissipation theorem (FDT). This FDT relation is discussed in details in the theoretical modeling section. The derivation of thermal magnetic noise is different from the thermal electronic noise. Ingvarsson *et al.* [29] ruled out the possibility of spin-dependent charging traps and magnetic

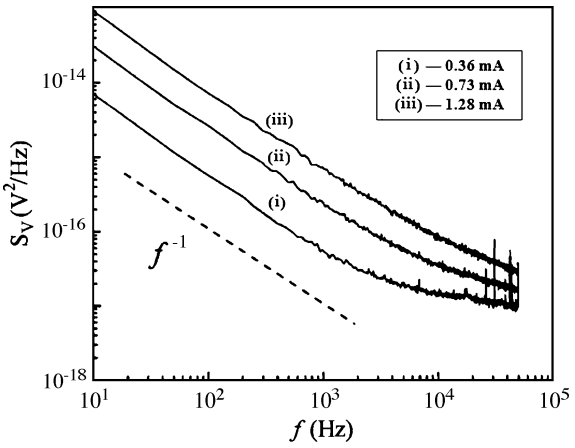

Fig. 2. A typical spectrum of $1/f$ noise. The noise power varies with biasing current in MTJs measured at $T = 2$ K. It increases with the dc current. The dash line is showing the $1/f$ slope. Reprinted with permission from [22].

impurities in the tunneling barrier. They suggested that thermal magnetic noise is originated from thermally excited hopping of domain walls between magnetic layers. This assumption was proved by Smith and Arnett [30]. Moreover they further proposed that the thermal magnetic noise is essentially frequency-independent and increases inversely with the free layer volume of MR sensors [30].

E. $1/f$ *Noise*

Another important noise source in MTJs is $1/f$ noise which is also known as flicker noise or excess noise. It can be found in various conductors and electronic devices that the spectral density of current increases inversely proportional to frequency in low-frequency regime [31]. Unlike white noise, $1/f$ noise is frequency-dependent. Its voltage power spectrum followed a $1/f$-like slope at low-frequency regime and the voltage power increases with biasing current as shown in Fig. 2. The spectrum density of $1/f$ noise is much larger than the thermal electronic noise and shot noise at low frequency. The mechanisms of $1/f$ noise in MTJs system can be categorized by two components: the electronic part and the magnetic part. They are named as electronic $1/f$ noise and magnetic $1/f$ noise respectively.

1) Electronic $1/f$ *Noise:* The origin of electronic $1/f$ noise can be attributed to charge trapping of electrons in barriers and between interfaces of tunnel junctions [32]–[34]. When current flows through MTJs, some of the charges become immobilized at the defects in the barriers and the mobility of carriers is slowed down. Subsequently the transmission processes of electrons disrupt each other. It was experimentally verified that highly crystallized tunnel barrier does not only enhance the TMR ratio but also mitigate the effect of $1/f$ noise in MTJs [35]. This effect probably ascribes to the reduced number of defects in the tunneling barriers and enhanced quality of interfaces between the thin films.

The electronic $1/f$ noise spectrum level can be evaluated by Hooge parameter [36] which is defined by

$$\alpha_{elec} = AfS_V^{elec.1/f}/V^2 \tag{3}$$

where $S_V^{elec.1/f}$ is the measured power spectrum of electronic $1/f$ noise, A is the junction area, f is the frequency and V is the voltage across the junction. The empirical and material-specific Hooge parameter was originally approximated by Hooge based on large numbers of experimental data on the magnitude of $1/f$ noise in semiconductor and metal films [37]. The Hooge parameter is utilized to parameterize the noise level of electronic $1/f$ noise. In MTJs, the value of α_{elec} changes with resistance-area (RA) product [22], [38]. Both Al_2O_3 and MgO MTJs exhibit comparatively large α_{elec} with larger RA [39]–[41]. α_{elec} also decreases with the biasing voltage of a junction [38]. It exhibits a lower value when the MTJs is treated with annealing process or fully biased in either parallel or anti-parallel configuration [21], [42]. Therefore, the Hooge parameter depends on various parameters (e.g. RA, TMR, and biasing conditions) of MTJs.

Table I shows the reported experimental values of Hooge parameter published in recent years. We can observe some general trends from Table I that α_{elec} changes with the RA, TMR, and biasing configurations. From the data in Table I, we plotted Fig. 3 showing the relations between (a) Hooge parameter and RA, and (b) Hooge parameter and TMR. As shown in Fig. 3(a), the value of α_{elec} generally increases with the RA. In Fig. 3(b), α_{elec} decreases with the TMR. Moreover, from both Figs. 3(a) and (b), we can observe that, overall speaking, the Al_2O_3 MTJs reveal larger electronic $1/f$ noise than MgO MTJs. On the other hand, as illustrated in Table I, the Hooge parameter varies with different biasing conditions including field biasing configurations (parallel or anti-parallel) and voltage biasing configurations (positive or negative). Almeida *et al.* [38] studied the dependency of Hooge parameter on the bias voltage systematically. It was pointed out that α_{elec} in parallel configuration is smaller than that in anti-parallel configuration. In addition, for the same parallel (or anti-parallel) configuration, α_{elec} in high biasing voltage is smaller than that in low biasing voltage. It was also noticed in their study that, although α_{elec} decreases with the biasing voltage of a junction, it is independent of the polarity of the bias voltage.

2) Magnetic $1/f$ *Noise:* Besides the electronic $1/f$ noise, magnetic fluctuation is observed as well in low-frequency regime. Its noise power spectrum is also found to be increasing with decreasing frequency. This magnetic fluctuation is associated with the magnetization alignment switching status at the interface between pinned layer and free layer [52], [53]. This fluctuation is different from the one induced by external magnetic field. Instead it represents the noise provoked in the direction of internal magnetizations. The maximum value of power density always appears when the ferromagnetic layers are switching in directions [52]. The magnetic $1/f$ noise can be attributed to the magnetization domain hopping between the metastable ripple states, resulting in the phenomenon of noise baseline shift [13], [54]. Such hopping process will affect the value of susceptibility of the free layer and provoke magnetic $1/f$ noise in the MTJs.

F. Random Telegraph Noise (RTN)

Random telegraph noise (RTN) was first systematically studied on double-gated junction field-effect transistors (JFETs) by Kandiah and Whiting in 1978 [55]. They found that RTN was generated by a defect center of charging and discharging process. Subsequently, RTN was discovered in various types

TABLE I
THE REPORTED EXPERIMENTAL VALUES OF HOOGE PARAMETER AT 300 K

Source of data	Barrier Material	Annealing Temperature (°C)	RA ($k\Omega\cdot\mu m^2$)	TMR ratio (%)	Hooge parameter (10^{-10} μm^2) in parallel configuration	Hooge parameter (10^{-10} μm^2) in anti-parallel configuration
[34]	Al_2O_3	N/A	4800	26.5	700.0	1500.0
[34]	Al_2O_3	N/A	7800	34.9	2000.0	3000.0
[34]	Al_2O_3	N/A	20500	33.1	5500.0	8000.0
[34]	Al_2O_3	N/A	37900	30.6	6500.0	9000.0
[34]	Al_2O_3	N/A	93600	26.7	1200.0	1600.0
[34]	Al_2O_3	N/A	114700	24.6	230.0	280.0
[39]	Al_2O_3	N/A	N/A	28	1500.0	4000.0
[40]	Al_2O_3	N/A	1500	35	20.0	N/A
[40]	Al_2O_3	N/A	10000	50	400.0	N/A
[40]	Al_2O_3	N/A	100000	7	1000.0	N/A
[43]	Al_2O_3	280	1500	41	32.0	N/A
[44]	Al_2O_3	250	30000	58	2000.0	N/A
[44]	Al_2O_3	250	40	58	20000.0	N/A
[45]	MgO	300	7000	20	20000.0	30000.0
[46]	MgO	360	0.15	130	22.0	22.0
[47]	MgO	360	0.15	100	8.2	N/A
[48]	MgO	375	N/A	235	2.5	5.0
[38]	MgO	330	40	90	2.5 (0.2 *V*); 4.0 (0.0003 *V*)	3.2 (0.4 *V*); 12.0 (0.001 *V*)
[38][a]	MgO	330	40	80	4.2 (0.40 *V*); 12.0 (0.7 *V*)	1.5 (0.0007 *V*); 80.0 (0.002 *V*)
[38]	MgO	330	0.6	150	1.1 (0.6 *V*); 2.1 (0.01 *V*)	2.2 (0.6 *V*); 11.0 (0.01 *V*)
[38]	MgO	330	7	125	1.7 (0.8 *V*); 4.2 (0.05 *V*)	3.0 (0.9 *V*); 30.0 (0.01 *V*)
[38]	MgO	330	50	167	1.2 (1.0 *V*); 3.0 (0.05 *V*)	11.0 (1.0 *V*); 120.0 (0.02 *V*)
[39]	MgO	N/A	700	122	40.0	N/A
[39]	MgO	N/A	1000	110	30.0	N/A
[39]	MgO	N/A	1500	43	20.0	N/A
[39]	MgO	N/A	6000	42	10.0	N/A
[49]	MgO	380	25-150	100	10.00	N/A
[49]	MgO	380	25-150	275	1.60	N/A
[49]	MgO	430	25-150	20	60.0 (0.3 V); 70.0 (-0.3 V)	N/A
[49]	MgO	430	25-150	100	6.0 (0.3 V); 6.0 (-0.3 V)	N/A
[49]	MgO	430	25-150	270	3.0 (0.3 V); 3.0 (-0.3 V)	N/A
[49]	MgO	430	25-150	275	1.6 (0.4 V); 1.6 (-0.4 V)	N/A
[38]	MgO	330	40	100	1.20 (0.6 V); 1.15 (-0.6 V)	2.61 (0.6 V); 2.74 (-0.6 V)
[38][a]	MgO	330	70	80	2.40 (0.6 V); 2.09 (-0.6 V)	19.0 (0.6 V); 17.0 (-0.6 V)
[38]	MgO	330	50	90	1.40 (0.8 V); 1.30 (-0.8 V)	17.0 (0.8 V); 18.0 (-0.8 V)
[50][b]	MgO	N/A	40	157	0.5 (0.4 V); 0.6 (-0.7 V)	3.0 (0.4 V); 0.2 (-0.7 V)
[51]	MgO	Unannealed	N/A	10	2.20	N/A
[51]	MgO	250	N/A	90	2.30	5.00
[51]	MgO	300	N/A	190	3.30	N/A
[51]	MgO	375	N/A	220	2.30	N/A

[a] Double barriers;

[b] Epitaxial MTJs, doped with carbon in the barrier;

N/A-Information not available;

The number in the parenthesis represents the biasing voltage.

of semiconductor devices. In MTJs, after eliminating magnetic noise by saturating the junctions with external magnetic field, RTN was observed intertwining with electronic $1/f$ noise in low-frequency regime and it became more obvious with the increase of biasing current [51]. Fig. 4(a) shows a typical voltage spectrum of RTN in the frequency domain. The RTN increases with the biasing current. Additionally, in the time domain, the spectrum reveals random step-like spikes with high and low states between distinct voltage levels, as presented in Fig. 4(b). This complicated noise behavior is created by the superposition of multilevel amplitude fluctuations due to the trapping centers. Therefore, RTN in tunneling junctions can be explained by repeated random capture of one electron into a single trap and emission of this electron from the trap [31].

Another explanation of RTN is thermal fluctuation of magnetization in free layer. Scola *et al.* [48] observed that the RTN can be eliminated by proper annealing and they attributed this phenomenon to the decrease of fluctuating magnetic domains in the electrodes. After annealing, the magnetic layers become better crystallized, resulting in the decline of magnetic fluctuations. Meanwhile, Hardner *et al.* [54] and Han *et al.* [56] ascribed RTN to the motions of domain walls and magnetic spin transfer effect [57], which are both caused by random magnetization fluctuations in the metastable states of free layers. Furthermore, Xi *et al.* [58] investigated the output voltage fluctuations of RTN in time- and frequency-domains by using the Stoner-Wohlfarth model which assumes a single-domain free layer magnetization. Their research results demonstrated that thermal activation can

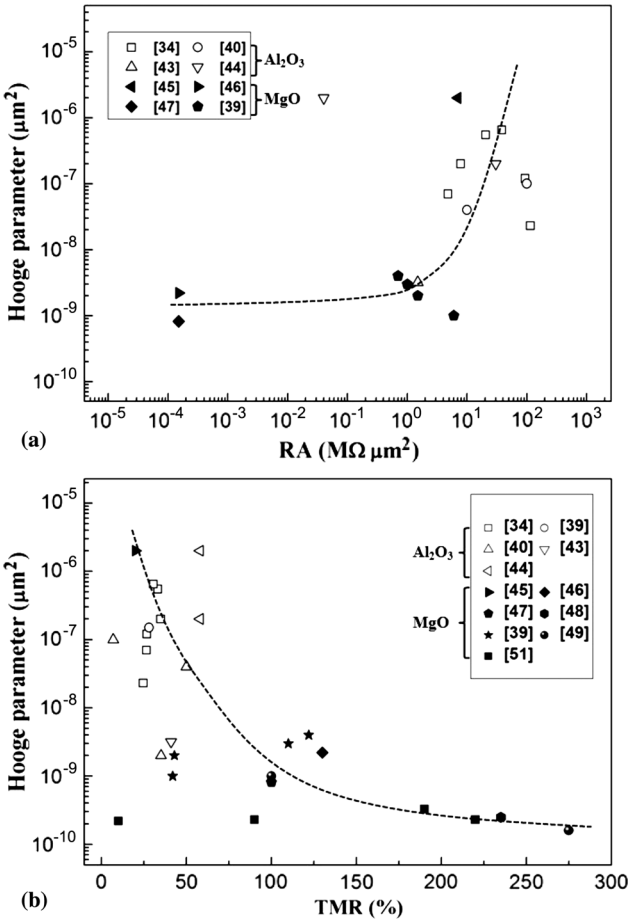

Fig. 3. Plots of the Hooge parameter (in parallel configuration) with RA and TMR. The data are from Table I. The open symbols represent Al_2O_3 MTJs and solid symbols represent MgO MTJs. The dashed lines are the guides for eyes. (a) Hooge parameter versus RA. The Hooge parameter reveals an increasing tendency with RA. (b) Hooge parameter versus TMR. The Hooge parameter generally decreases with TMR.

induce the voltage fluctuations and thus RTN in MTJs. Gokce *et al.* [41] and Egelhoff *et al.* [13] also deduced RTN to be connected with the metastability in the magnetization of a free layer. In summary, all these works attribute the origins of RTN to the fluctuations in the magnetic free layers and this approach provides a reasonable explanation for the observation that the noise is reduced after annealing. The theoretical modeling of RTN is discussed in Section III.

III. Theoretical Modeling of MTJ Noises

Theoretical modeling of noise provides an effective mathematical tool to investigate noise behaviors in MTJs. The influences of individual limiting parameter for each noise source in MTJs can be intuitively observed. Researchers can simulate and predict the noise spectrum with the assistance of the theoretical modeling. A MTJ sensor design can thus be optimized according to the simulation results. In this section, theoretical models of MTJ noises are presented.

A. Amplifier Noise

An amplifier is needed for amplifying the signal level for data acquisition and spectral measurement. However, as discussed in the previous section, the amplifier itself is a noise source that

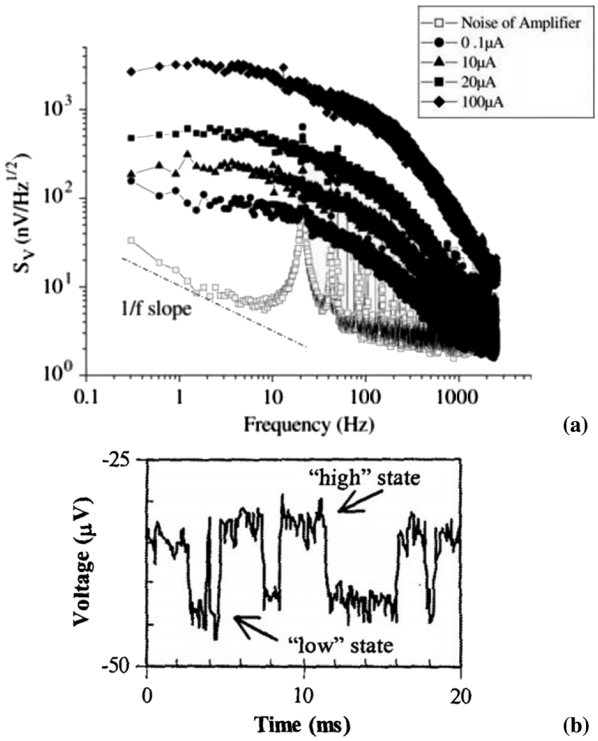

Fig. 4. Typical noise spectra of random telegraph noise (RTN). (a) Noise voltage spectrum in the frequency domain. The RTN becomes more obvious with the increase of biasing current. Reprinted with permission from [51]. (b) The variation of the noise voltage in the time domain showing discrete high and low states. Reprinted with permission from [54].

contributes to the noise floor and deteriorates the SNR. By establishing a noise measurement setup like Fig. 5, the amplifier noise can be characterized by short circuiting the MTJs in the bridge. The noise power spectrum shown in the spectrum analyzer is then the amplifier noise power spectrum S_V^{Amp}. Its field noise power spectrum S_B^{Amp} can be found from the voltage noise power spectrum S_V^{Amp} by the following equation:

$$S_B^{Amp} = \left(\frac{dB}{dV}\right)^2 S_V^{Amp} \tag{4}$$

where dB/dV is the reciprocal of the sensor voltage response to external magnetic field.

B. Thermal-Shot Noise

Shot noise in mesoscopic conductors was systematically studied by Landauer *et al.* [59]. Their research results showed that, besides the shot noise, thermal noise is also significant in the mesoscopic devices. Thermal-equilibrium noise is due to independent electron emission. Equation (1) satisfactorily explains the general current fluctuations in tunneling junctions; however, it fails to describe the current fluctuations caused by thermal energy. In order to take into account the effect of thermal energy, an expression (from [60]) of voltage power for thermal-shot noise is given by

$$S_V^{therm-shot} = 2eIR^2 \coth\left(\frac{eV}{2k_BT}\right) \tag{5}$$

where V is the dc bias voltage across the junction. Equation (5) well describes the density spectra of both thermal and shot

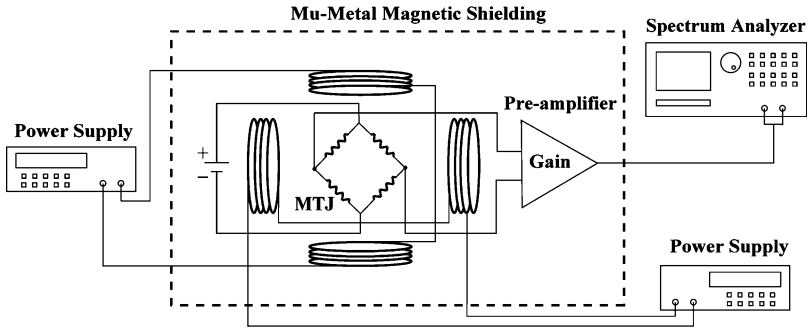

Fig. 5. Schematic diagram of a MTJ noise measurement setup. MTJ sensors are arranged in a Wheatstone bridge configuration. Low-noise instrumentation preamplifier is used for signal amplification. The measurement circuit is shielded in a mu-metal magnetic shielding. A spectrum analyzer is used for capturing the noise spectrum.

TABLE II
MATHEMATICAL FORMULAE OF THERMAL MAGNETIC NOISE POWER $S_M^{therm.mag.}$ BASED ON FDT

Reference	Noise formula	Definition of terms
[28]	$S_M^{therm.mag.} = \frac{2k_BT\chi''(f)}{\pi\Omega f}$	Ω is the volume of free layer $\chi''(f)$ is the imaginary dissipative out-of-phase susceptibility driven by applied fields M_S is the saturation magnetization of the free layer per unit volume μ_0 is the vacuum permeability of free layer
[30]	$S_M^{therm.mag.} = \frac{2k_BT\chi''(f)}{\pi\Omega f M_S^2}$	
[13]	$S_M^{therm.mag.} = \frac{2k_BT\chi''(f)}{\pi\Omega\mu_0 f}$	
[62]	$S_M^{therm.mag.} = \frac{2k_BT\chi''(f)}{\pi\Omega f M_S^2\mu_0}$	
[29] [22]	$S_M^{therm.mag.} = \frac{2k_BT\chi''(f)}{\pi\mu_0 f}$	

noises in MTJs. When the bias voltage is low $eV \ll k_BT$, (5) is equivalent to thermal electronic noise, $S_V^{therm.elec.} = 4k_BTR$. On the other hand, at low temperature or high voltage biases $eV \gg k_BT$, (5) approaches to shot noise, $S_V^{shot} = 2eIR^2$. This expression is in good agreement with the general descriptions of thermal electronic noise and shot noise.

When considering the influence of Fano factor (F), the final expression of voltage power for thermal-shot noise is given by the following equation [26], [27]

$$S_V^{therm-shot} = 4(1-F)\cdot k_BTR + 2F\cdot eIR^2\coth\left(\frac{eV}{2k_BT}\right). \tag{6}$$

If the tunneling junction undergoes a full shot noise $(F = 1)$, the results of (5) and (6) are the same. Conversely, if the thermal-shot noise is enhanced $(F > 1)$ or suppressed $(F < 1)$, the results of (5) and (6) are different.

C. Thermal Magnetic Noise

The magnetization fluctuations in MTJs contribute to the total noise of the device. The fluctuation effect can be explained by fluctuation-dissipation theorem (FDT). FDT describes a general relation between the internal fluctuation of a thermal system to an external disturbance [61]. FDT is widely used for predicting the characteristics of the intrinsic noise and it is used as the basic formula for the analysis of thermal fluctuations of a MTJ system. The mathematical formulae based on FDT for describing the noise spectra of thermal magnetic noise in MR devices were published by several groups [22], [28]–[30], [62], [63] in different expressions (see Table II).

Although the equations listed in Table II do not reach a single form, they tend to associate the origins of thermal magnetic noise to temperature (T), magnetic susceptibility (χ''), magnetization (M_S), and the volume of MTJ free layers (Ω). Based on the FDT-related equation, Egelhoff *et al.*. attributed the variation of imaginary susceptibility $\chi''(f)$ to the uniform rotation of the free layer magnetization via spin-dependent tunneling effect [13]. They proposed a method for calculating the power spectrum of thermal magnetic noise by employing the Gilbert damping parameter and Gyromagnetic ratio. The field power is given by the following equation

$$S_M^{therm.mag.} = \frac{4k_BT\mu_0\alpha_G}{\Omega\gamma M_S} \tag{7}$$

where α_G is the Gilbert damping parameter, γ is Gyromagnetic ratio for an electron. The details of derivations of the equation can be found in [13].

D. Electronic $1/f$ Noise

The electronic $1/f$ noise has been extensively studied in electronic devices over the past decades [32]–[35]. Most of the

experimental results showed a $1/f$-type slope in the low-frequency regime of a noise spectrum. The electronic 1/f noise power of MTJs can be described by

$$S_V^{elec.1/f} = \alpha_{elec}\frac{V^2}{Af^\beta} \tag{8}$$

where A is the junction area of a MTJ, V is the applied voltage across the junctions, f is the frequency, and α_{elec} is the electronic $1/f$ Hooge parameter. β is the exponent of electronic $1/f$ noise spectrum and its value fluctuates in the range of 0.6–2.0 [39], [40], [49], [64]–[66]. The value of β varies for different MTJs.

E. Magnetic $1/f$ Noise

Besides the thermally activated mechanism, the susceptibility is also affected by the magnetization hopping between the metastable ripple states. Egelhoff *et al.* [13] deduced the equation for describing the magnetic $1/f$ noise from FDT relation, the field power spectrum is

$$S_B^{mag.1/f} = \frac{2B_{sat}\alpha_{mag}}{\Omega f} \tag{9}$$

where $\alpha_{mag} = k_BT[\chi''\ \chi']/\pi M_S$, χ' is the real part of the out-of-phase susceptibility and B_{sat} is the saturation field of free layer. α_{mag} is the magnetic $1/f$ noise parameter and its value can be determined empirically from the noise spectrum of the MTJs. α_{mag} can be used for evaluating the noise level of magnetic $1/f$ noise which is comparable to α_{elec} of the electronic $1/f$ noise.

Ozbay *et al.* [62] proposed another mathematical expression for depicting the magnetic noise, given by

$$S_B^{mag} = \frac{\alpha'_{mag}}{\mu_0^2\Omega f}\left(\frac{1}{R}\frac{dR}{dH}\right)^{-2} \tag{10}$$

where $\alpha'_{mag} = [\chi''/\chi'](k_BT/\pi\mu_0 M_S)(\Delta R/R)((1/R)(dR/dH))$, $(1/R)(dR/dH)$ is derived from the MR transfer curve [22], [29]. α'_{mag} can also be used for evaluating the magnetic noise level. However, α'_{mag} is different from α_{mag} because (10) depicts both magnetic $1/f$ noise and thermal magnetic noise.

Similar to thermal magnetic noise, magnetic $1/f$ noise is also dependent on magnetic field. However, the prominent difference between these two magnetic originated noises is that the latter contains a $1/f$ component in the equation and it is frequency-dependent. The former is frequency-independent and it can be considered as white noise [30].

F. Random Telegraph Noise (RTN)

RTN is not always obvious and it is shadowed by $1/f$ noise in the low-frequency regime. The voltage spectrum of RTN is Lorentzian and it is given by

$$S_V^{RTN} = \frac{S_0}{1+(f/f_0)^2} \tag{11}$$

where S_0 is the frequency-independent portion of S_V^{RTN} observed at f, f_0 is the characteristic roll-off frequency described by $f_0 = (2\pi\tau)^{-1}$, and τ is the relaxation time of Lorentzian fluctuations. The voltage power spectrum of white RTN can be isolated from frequency-dependent $1/f$ noise with (11).

G. Total System Noise

As mentioned in Section II, all of the noise sources in MTJs are incoherent. The total system noise is the summation of all the uncorrelated noise sources mentioned above. The total field noise spectrum is given by

$$S_B^{Total} = \left(\frac{dB}{dV}\right)^2\left[S_V^{Amp}+S_V^{therm-shot}+S_V^{elec.1/f}+S_V^{RTN}\right] + S_B^{therm.mag.} + S_B^{mag.1/f}. \tag{12}$$

IV. Methods for Eliminating Noises

Researchers have made great efforts on studying noises in order to eliminate the noises in MTJ sensors. There are various ways to reduce the noise floor in MTJs such as optimizing MTJ dimensions and structures, biasing conditions, operation temperature, etc. Methods for suppressing different noise sources are discussed in this section.

A. Ambient Noise and Amplifier Noise

The external environment and the amplifier can bring noises to the sensor system. The temperature variation of the ambience can lead to thermal instability which agitates domain-wall motions, creating low-frequency noise in MTJs. A Wheatstone bridge configuration can be used to alleviate the effect of thermal drift [1], [13], [67], [68]. It can also solve the problem of dc offset. Another way to reduce system noise is to shield the measurement system with a magnetic shielding (as shown in Fig. 5). A magnetic shielding is usually made of mu-metal (alloy of Ni-Fe-Cu-Mo) [69] for its soft magnetic property. Mu-metal has very high relative permeability ($\sim 10^5$) [69] and it can effectively divert the external magnetic field to go along the shielding instead of interrupting the MTJ sensors inside the shielding. It is an effective means to reduce the disturbance caused by external magnetic field. Amplifier noise is inevitable because of the connections of preamplifiers in a bridge-measurement circuit for amplifying the sensor signal. One way to curtail amplifier noise is to use low-noise instrumentation amplifiers (e.g. Femto DLPVA-100-BLN-S) and utilize batteries as the power source so as to avoid the noise from the mains [46], [67]. As such, the voltage and current noises of the amplifier can be suppressed to an acceptable level.

B. Thermal-Shot Noise

The thermal-shot noise is white noise and it sets the noise floor in both low- and high-frequency regimes. The application of a bridge configuration is effective in reducing the thermal-shot noise by reducing the dc offset and thermal drift. Moreover, from (5), we can infer that thermal-shot noise can be reduced by increasing the voltage bias across the tunneling junction and lowering the temperature of the working environment.

These relations are well supported by the experimental data [25]. However, tradeoff needs to be made because increasing biasing voltage will reduce TMR ratios.

C. Magnetic Noises

Thermal magnetic noise and magnetic $1/f$ noise are both magnetically derived noise. Their noise levels are closely related to the material properties of MTJs. As discussed in the previous sections, thermal magnetic noise is associated with the free layer volume of a MTJ [43], [62]. Equation (7) provides the insight that thermal magnetic noise can be reduced by increasing the free-layer volume. This can be realized by increasing the junction area or the thickness of magnetic layers. Similarly, the magnetic $1/f$ noise reduces with the thickness of magnetic free layers and thus it can also be eliminated by increasing the free-layer thickness [70], [71]. In addition, minimizing the saturation field of the free layer B_{sat} can reduce the magnetic $1/f$ noise as well. It can be achieved through the method of fixing the magnetic domains of the free layer by reducing the free-layer thickness [70], [72]. However, this will decrease the TMR ratios. Moreover, reducing free-layer thickness decreases free-layer volume which will increase the magnetic $1/f$ noise according to (9) and (10). Therefore, it is a tradeoff regarding the free-layer thickness for minimizing the magnetic noises. Applying a hard-axis magnetic field can eliminate the hysteresis in TMR loops and also reduce magnetic noises by restraining magnetization fluctuation in magnetic layers in MTJs. Nevertheless, the hard-axis field will deteriorate the TMR ratios [12], [64] and thus it needs to be compromised.

D. Electronic $1/f$ Noise

Electronic $1/f$ noise was reported to be curtailed by several methods. One of them is increasing the number of MTJ junctions in series or parallel. Tondra *et al.* [73] pointed out that increasing the number of MTJ elements can effectively increase the sensor SNR. Guerrero *et al.* [74] enhanced the sensitivity up to 16.2 $\mathrm{nT/Hz^{1/2}}$ by using MTJ arrays in series and in parallel. Another method to reduce electronic $1/f$ noise is chopping the magnetic signal by making use of the nonlinear response of the field transfer curve. Jander *et al.* [75] explored different chopping methods and their results showed a 20% reduction of noise power with a parallel chopping technique in low-frequency domain. An alternative way to eliminate electronic $1/f$ noise is to use microelectromechanical system (MEMS) magnetic flux concentrators. Edelstein *et al.* [76] designed a MEMS-based magnetic flux concentrators for reducing the electronic $1/f$ noise (Fig. 6). The flux concentrators made of permalloy are deposited on MEMS flaps. The MEMS flaps can be driven into oscillation by applying ac voltage to the electrostatic comb drives. A MTJ sensor is placed at the middle of the pair of flaps. The MEMS flux concentrator shifts the operating point of the MTJ sensor to the high-frequency regime to avoid the $1/f$ noise which is dominant in the low-frequency regime. It also helps in reducing magnetic noise by enhancing the magnetic field passing through the MTJ sensors. Guedes *et al.* [77] proposed a similar structure of MEMS flux concentrator but it is based on the mechanical motion of a cantilever. The device structure is shown in Fig. 7. A magnetic flux guide is located on the MEMS

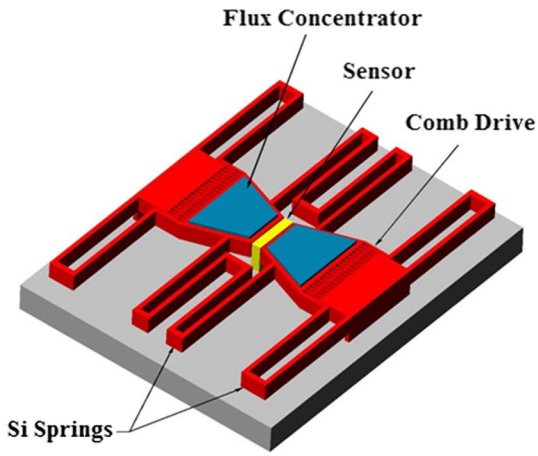

Fig. 6. Schematic drawing of the basic structure of MEMS magnetic flux concentrator proposed by Edelstein *et al*. [76]. The flux concentrator was deposited on the MEMS structure which can be driven into oscillation by applying an ac voltage. The Si springs ensure the flux concentrators on both sides to oscillate at the same frequency. Reprinted with permission from [76].

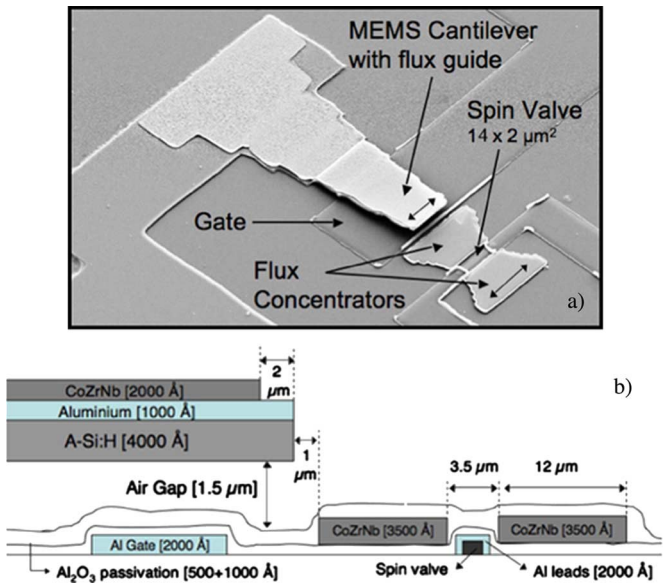

Fig. 7. Illustrations of MR sensor with MEMS device. (a) SEM micrograph of the fabricated sensor system with the MEMS cantilever, 200 nm thick magnetic flux guide, and the MTJ spin valve sensor. The double-headed arrows indicate the direction of easy axis. (b) Cross-sectional view of the device. Reprinted with permission from [77].

microcantilever. When applying an ac voltage at frequency f to the gate electrode, the periodical electrostatic force drives the cantilever to oscillate with a frequency of $2f$. This design also aims at shifting the operating frequency of MTJ sensor to a higher frequency to avoid the $1/f$ noise in the low-frequency regime.

These methods can potentially greatly reduce the electronic $1/f$ noise. However, there are some technical difficulties needed to be overcome. Increasing the number of MTJs elements or applying the chopping techniques for reducing electronic $1/f$ noise at low-frequency regime still face the problems of high power consumption and excessive noise at high-frequency regime respectively. MEMS magnetic flux concentrators have the problem of requiring large working voltage in order to obtain the necessary oscillation amplitude of

TABLE III
EMPIRICAL AND SIMULATED RELATIONS BETWEEN DIFFERENT PARAMETERS AND NOISE POWERS IN MTJ SENSOR SYSTEMS

Parameters	Empirical data							Simulation					
	$S_V^{therm-shot}$	$S_V^{elec.1/f}$	$S_B^{therm.mag.}$	$S_B^{mag.1/f}$	S_V^{RTN}	S_B^{Total}	Source of data	$S_V^{therm-shot}$	$S_V^{elec.1/f}$	$S_B^{therm.mag.}$	$S_B^{mag.1/f}$	S_V^{RTN}	S_B^{Total}
V	↑↓	↑↓	N/A	N/A	↑↓	↑↓	[25] [51]	↑↓	NR	NR	NR	NR	↑↓
N	↑↓	↑↓	↑↓	↑↓	↑↓	↑↓	[73] [74]	↑↓	↑↓	↑↓	↑↓	NR	↑↓
A	↑↓	↑↓	↑↓	↑↓	↑↓	↑↓	[23] [38]	↑↓	↑↓	↑↓	↑↓	NR	↑↓
B_{sat}	↑↑	↑↑	↑↑	↑↑	↑↑	↑↑	[30] [65]	↑↑	↑↑	NR	NR	NR	↑↑
TMR	↑↓	↑↓	N/A	N/A	↑↓	↑↓	[39] [14]	↑↓	↑↓	NR	NR	NR	↑↓
G	↑↓	↑↓	↑↓	N/A	N/A	↑↓	[76] [77]	↑↓	↑↓	↑↓	NR	NR	↑↓
T_{op}	↑↑	N/A	↑↑	N/A	↑↓	↑↑	[14] [29]	↑↑	NR	↑↑	NR	NR	↑↑
RA	↑↓	↑↑	N/A	N/A	↑↓	↑↓	[23] [38]	↑↓	NR	NR	NR	NR	↑↓
t_{FL}	N/A	N/A	↑↓	↑↓	↑↓	↑↓	[70] [72]	NR	NR	↑↓	↑↓	NR	↑↓

↑↑—Two parameters vary in the same direction
↑↓—Two parameters vary in the opposite direction
N/A-Information not available
NR-No relation between the two parameters in the simulation

the MEMS structures, and their efficiency is low [78], [79]. For example, the design with a MEMS cantilever has a low level of modulation efficiency of around 0.0019% [80]. Although these approaches still need further improvement, they provide some feasible means for reducing electronic $1/f$ noise.

E. RTN

RTN is shadowed by $1/f$ noise in low-frequency regime. As frequency increases, $1/f$ noise reduces. Then RTN becomes more obvious and emerges as a bump in the noise spectrum (Fig. 4(a)). On the other hand, as we can see from the several noise spectra in Fig. 4(a), RTN increases with biasing current. Almeida *et al.* pointed out that RTN's magnitude is dependent on RA value and biasing voltage [38]. Their experimental results indicated that MTJs with larger RA product and lower bias voltage do not exhibit RTN. The performance of RTN is also related to MTJ annealing conditions. Scola *et al.* reported that RTN can be eliminated by annealing the samples at 375°C for 90 min [48]. The annealing process reshapes the distribution of energy barriers and the magnetization configuration of domains, thus the magnetic layers of MTJs become more optimized [56], [57].

F. Discussion

There are various factors influencing the noises in MTJs. They are biasing voltage (V), number of MTJ elements (N), free-layer volume (determined by junction area (A) and free-layer thickness (t_{FL})), operating temperature (T_{op}), gain of the concentrator (G), etc. Previously, we theoretical derived and calculated the influence of each parameter on MTJ noise level [13], [81]. Based on these theoretical derivations, a simulation tool called magnetic sensor design tool (MSDT) was developed [81]. This simulation tool enables us to predict the influence of each parameter on MTJ noise level. We compared the published experimental results with the simulation results. Both the empirical and simulated relations between MTJ sensor design parameters and noise powers are presented in Table III.

We can observe from Table III that the simulation results and the experimental data generally agree with each other. Although there is no major contradiction, there are discrepancies between the empirical and simulated results in the relations between V and electronic $1/f$ noise $(S_V^{elec.1/f})$, B_{sat} and magnetic noise $(S_B^{therm.mag.}$ and $S_B^{mag.1/f})$, and RA and electronic $1/f$ noise $(S_V^{elec.1/f})$. More research efforts are needed to resolve these discrepancies. Moreover, the theoretical model can be further refined to distinguish the power spectra of RTN (S_V^{RTN}) and magnetic $1/f$ noise $(S_B^{mag.1/f})$.

V. CONCLUSION AND OUTLOOK

A. Conclusion

Noises exist in MTJs and they limit the sensitivity of MTJ sensors. The MTJ noises contain the electronic and magnetic information and identifying the origins of these noises can help us to understand the electron transport and magnetic dynamics. This enables researchers to establish mathematical models for various kinds of MTJ noises and optimize a MTJ sensor design before the actual fabrication.

In conclusion, we reviewed the noise sources in MTJs and endeavor to seek effective approaches to reduce the noises of MTJ sensors. Both theoretical analysis and mathematical modeling are presented to illustrate the relations between noise powers and each individual parameter of a MTJ sensor system. We compared the published experimental results with the simulation results. In general, the simulation results based on the mathematical models of MTJ noises agree with the published experimental results. However, there exist some discrepancies and more research studies are needed to enhance our understanding on MTJ noises. In addition, some feasible methods for eliminating MTJ sensor noises are discussed. Annealing can enhance both the TMR and noise performance by optimizing the multilayer interface roughness, enhancing thermal stability of magnetic layers, and removing barrier defects. Improving the quality

of tunneling barrier is critical for improving MTJ sensor performance. The application of MEMS flux concentrators can potentially bring significant improvement to the sensor capability of detecting ultra-low magnetic field in low-frequency regime. However, some of these methods for eliminating noises need tradeoff in sensor design. For example, although the saturation field of MTJs can be reduced (thus MTJ sensitivity is enhanced) by decreasing the free-layer volume, the free-layer thickness should not be smaller than a critical thickness; otherwise the TMR will suffer and magnetic noise will increase greatly. The application of transverse bias field can restrain magnetic fluctuations and thus reduce magnetic noise; however, it is at the expense of TMR ratios. Suppressing thermal-shot noise can be achieved by raising the biasing current; however, this elicits RTN problem and increases power consumption of MTJ sensors. These methods will require further studies to find compromised parameters for an optimized MTJ sensor system design.

B. Perspective and Outlook

MTJ sensors offer a possibility for magnetometer miniaturization which is compact-in-size, less power consumption, more sensitive, and lower in cost. The future work on MTJ magnetic field sensors will be likely focusing on increasing the TMR and SNR by optimizing the MTJ structures and material properties. The final performance of MTJ sensors is not solely determined by TMR. The minimum detectable field is determined by the total noise floor. Therefore, the study on noise analysis in MTJs is critical for sensor design in the coming decade. A promising research area is to integrate MTJ sensors with MEMS oscillating flux concentrators to eliminate $1/f$ noise and the effect of dc offset. The critical challenge of this approach remains in lowering the driving voltage, improving modulation efficiency, and developing better chip bonding and packaging technique. If the $1/f$ noise can be reduced by adding an external MEMS flux concentrator, then the ultimate noise floor will probably be set by white noise. Thus, the next-stage work will be in minimizing the white noise floor for enhancing the detectivity of MTJ sensors.

ACKNOWLEDGMENT

This work was supported by the Seed Funding Program for Basic Research of the University of Hong Kong.

REFERENCES

[1] A. Edelstein, "Advances in magnetometry," *J. Phys.: Condens. Matter.*, vol. 19, pp. 165217–165244, 2007.
[2] M. Julliere, "Tunneling between ferromagnetic films," *Phys. Lett. A*, vol. 54, pp. 225–226, 1975.
[3] J. Mathon and A. Umerski, "Theory of tunneling magnetoresistance of an epitaxial Fe/MgO/Fe(001) junction," *Phys. Rev. B*, vol. 63, p. 220403, 2001.
[4] W. H. Butler, X.-G. Zhang, T. C. Schulthess, and J. M. MacLaren, "Spin-dependent tunneling conductance of Fe/MgO/Fe sandwiches," *Phys. Rev. B*, vol. 63, p. 054416, 2001.
[5] S. Ikeda, J. Hayakawa, Y. Ashizawa, Y. M. Lee, K. Miura, H. Hasegawa, M. Tsunoda, F. Matsukura, and H. Ohno, "Tunnel magnetoresistance of 604% at 300 K by suppression of Ta diffusion in CoFeB/MgO/CoFeB pseudo-spin-valves annealed at high temperature," *Appl. Phys. Lett.*, vol. 93, p. 082508, 2008.
[6] W. Shen, X. Liu, D. Mazumdara, and G. Xiao, "In situ detection of single micron-sized magnetic beads using magnetic tunnel junction sensors," *Appl. Phys. Lett.*, vol. 86, pp. 253901–253903, 2005.
[7] F. A. Cardoso, H. A. Ferreira, V. Chu, P. P. Freitas, D. Vidal, J. Germano, L. Sousa, M. S. Piedade, B. A. Costa, and J. M. Lemos, "Diode/magnetic tunnel junction cell for fully scalable matrix-based biochip," *J. Appl. Phys.*, vol. 99, p. 08B307-3, 2006.
[8] K. L. Phan, H. Boeve, F. Vanhelmont, T. Ikkink, F. de Jong, and H. de Wilde, "Tunnel magnetoresistive current sensors for IC testing," *Sens. Actuators, A*, vol. 129, pp. 69–74, 2006.
[9] D. Robbes, "Highly sensitive magnetometers—A review," *Sens. Actuators, A*, vol. 129, p. 86, 2006.
[10] M. Pannetier, C. Fermon, G. Le Goff, J. Simola, and E. Kerr, "Femtotesla magnetic field measurement with magnetoresistive sensors," *Science*, vol. 304, p. 1648, 2004.
[11] N. C. Currie, F. J. Demma, J. D. D. Ferris, R. W. McMillan, M. C. Wicks, and K. Zyga, "Imaging sensor fusion for concealed weapon detection," *Proc. SPIE*, vol. 2942, pp. 71–81, 1997.
[12] R. C. Chaves, P. P. Freitas, B. Ocker, and W. Maass, "MgO based picotesla field sensors," *J. Appl. Phys.*, vol. 103, pp. 07E931–07E933, 2008.
[13] W. F. Egelhoff, Jr, P. W. T. Pong, J. Unguris, R. D. McMichael, E. R. Nowak, A. S. Edelstein, J. E. Burnette, and G. A. Fischer, "Critical challenges for picoTesla magnetic-tunnel-junction sensors," *Sens. Actuators, A*, vol. 155, pp. 217–225, 2009.
[14] E. R. Nowak, R. D. Merithew, M. B. Weissman, I. Bloom, and S. S. P. Parkin, "Noise properties of ferromagnetic tunnel junctions," *J. Appl. Phys.*, vol. 84, pp. 6195–6201, 1998.
[15] S. Ingvarsson, G. Xiao, R. A. Wanner, P. Trouilloud, Y. Lu, W. J. Gallagher, A. Marley, K. P. Roche, and S. S. P. Parkin, "Electronic noise in magnetic tunnel junctions," *J. Appl. Phys.*, vol. 85, pp. 5270–5272, 1999.
[16] [Online]. Available: http://www.nist.gov/msel/metallurgy/magnetic_materials/magnetic_sensors.cfm
[17] J. B. Johnson, "Thermal agitation of electricity in conductors," *Phys. Rev.*, vol. 32, p. 97, 1928.
[18] H. Nyquist, "Thermal agitation of electric charge in conductors," *Phys. Rev.*, vol. 32, p. 110, 1928.
[19] W. Schottky, "Über spontane stromschwankungen in verschiedenen Elektrizitätsleitern," *Ann. Phys.*, vol. 362, pp. 541–567, 1918.
[20] C. Beenakker and C. Schonenberger, "Quantum shot noise," *Phys. Today*, vol. 56, pp. 37–42, 2003.
[21] L. Jiang, J. F. Skovholt, E. R. Nowak, and J. M. Slaughter, "Low-frequency magnetic and resistance noise in magnetoresistive tunnel junctions," *Proc. SPIE*, vol. 5469, pp. 13–27, 2004.
[22] L. Jiang, E. R. Nowak, P. E. Scott, J. Johnson, J. M. Slaughter, J. J. Sun, and R. W. Dave, "Low-frequency magnetic and resistance noise in magnetic tunnel junctions," *Phys. Rev. B*, vol. 69, p. 054407, 2004.
[23] R. Guerrero, F. G. Aliev, Y. Tserkovnyak, T. S. Santos, and J. S. Moodera, "Shot noise in magnetic tunnel junctions: Evidence for sequential tunneling," *Phys. Rev. Lett.*, vol. 97, p. 266602, 2006.
[24] P. K. George, Y. Wu, R. M. White, E. Murdock, and M. Tondra, "Shot noise in low-resistance magnetic tunnel junctions," *Appl. Phys. Lett.*, vol. 80, pp. 682–684, 2002.
[25] S. Garzon, Y. Chen, and R. A. Webb, "Enhanced spin-dependent shot noise in magnetic tunnel barriers," *Physica E*, vol. 40, pp. 133–140, 2007.
[26] K. Sekiguchi, T. Arakawa, Y. Yamauchi, K. Chida, M. Yamada, H. Takahashi, D. Chiba, K. Kobayashi, and T. Ono, "Observation of full shot noise in CoFeB/MgO/CoFeB-based magnetic tunneling junctions," *Appl. Phys. Lett.*, vol. 96, p. 252504-3, 2010.
[27] Y. M. Blanter and M. Buttiker, "Shot noise in mesoscopic conductors," *Phys. Rep.*, vol. 336, p. 1, 2000.
[28] H. T. Hardner, M. B. Weissman, M. B. Salamon, and S. S. P. Parkin, "Fluctuation-dissipation relation for giant magnetoresistive 1/f noise," *Phys. Rev. B*, vol. 48, p. 16156, 1993.
[29] S. Ingvarsson, G. Xiao, S. S. P. Parkin, W. J. Gallagher, G. Grinstein, and R. H. Koch, "Low-frequency magnetic noise in micron-scale magnetic tunnel junctions," *Phys. Rev. Lett.*, vol. 85, p. 3289, 2000.
[30] N. Smith and P. Arnett, "White-noise magnetization fluctuations in magnetoresistive heads," *Appl. Phys. Lett.*, vol. 78, pp. 1448–1450, 2001.
[31] S. Kogan, *Electronic Noise and Fluctuations in Solids*. Cambridge, U.K.: Cambridge University Press, 2008.
[32] M. E. Welland and R. H. Koch, "Spatial location of electron trapping defects on silicon by scanning tunneling microscopy," *Appl. Phys. Lett.*, vol. 48, pp. 724–726, 1986.
[33] M. B. Weissman, "1/f noise and other slow, nonexponential kinetics in condensed matter," *Rev. Mod. Phys.*, vol. 60, p. 537, 1988.

[34] E. R. Nowak, M. B. Weissman, and S. S. P. Parkin, "Electrical noise in hysteretic ferromagnet-insulator-ferromagnet tunnel junctions," *Appl. Phys. Lett.*, vol. 74, pp. 600–602, 1999.

[35] A. F. Md Nor, T. Daibou, M. Oogane, Y. Ando, and T. Miyazaki, "Boron effects on noise in magnetic tunnel junctions," *J. Magn. Magn. Mater.*, vol. 310, pp. 1917–1919, 2007.

[36] F. N. Hooge, "1/f noise," *Physica B+C*, vol. 83, pp. 14–23, 1976.

[37] F. N. Hooge, T. G. M. Kleinpenning, and L. K. J. Vandamme, "Experimental studies on 1/f noise," *Rep. Prog. Phys.*, vol. 44, p. 479, 1981.

[38] J. M. Almeida, P. Wisniowski, and P. P. Freitas, "Low-frequency noise in MgO magnetic tunnel junctions: Hooge's parameter dependence on bias voltage," *IEEE Trans. Magn.*, vol. 44, pp. 2569–2572, 2008.

[39] A. F. M. Nor, T. Kato, S. J. Ahn, T. Daibou, K. Ono, M. Oogane, Y. Ando, and T. Miyazaki, "Low-frequency noise in MgO magnetic tunnel junctions," *J. Appl. Phys.*, vol. 99, p. 08T306-3, 2006.

[40] W. K. Park, J. S. Moodera, J. Taylor, M. Tondra, J. M. Daughton, A. Thomas, and H. Bruckl, "Noise properties of magnetic and nonmagnetic tunnel junctions," *J. Appl. Phys.*, vol. 93, pp. 7020–7022, 2003.

[41] A. Gokce, E. R. Nowak, S. H. Yang, and S. S. P. Parkin, "1/f noise in magnetic tunnel junctions with MgO tunnel barriers," *J. Appl. Phys.*, vol. 99, p. 08A906-3, 2006.

[42] X. Liu and G. Xiao, "Thermal annealing effects on low-frequency noise and transfer behavior in magnetic tunnel junction sensors," *J. Appl. Phys.*, vol. 94, pp. 6218–6220, 2003.

[43] P. W. T. Pong, J. E. Bonevich, and J. W. F. Egelhoff, "Development of ultra-low magnetic field sensors with magnetic tunneling junctions," *Proc. SPIE*, vol. 6645, p. 66450B-12, 2007.

[44] J. Schmalhorst and G. Reiss, "Temperature and bias-voltage dependent transport in magnetic tunnel junctions with low energy Ar-ion irradiated barriers," *Phys. Rev. B*, vol. 68, p. 224437, 2003.

[45] R. Guerrero, F. G. Aliev, R. Villar, J. Hauch, M. Fraune, G. Guntherodt, K. Rott, H. Bruckl, and G. Reiss, "Low-frequency noise and tunneling magnetoresistance in Fe(110)/MgO(111)/Fe(110) epitaxial magnetic tunnel junctions," *Appl. Phys. Lett.*, vol. 87, pp. 042501–042503, 2005.

[46] J. M. Almeida, R. Ferreira, P. P. Freitas, J. Langer, B. Ocker, and W. Maass, "1/f noise in linearized low resistance MgO magnetic tunnel junctions," *J. Appl. Phys.*, vol. 99, p. 08B314, 2006.

[47] R. C. Chaves, P. P. Freitas, B. Ocker, and W. Maass, "Low frequency picotesla field detection using hybrid MgO based tunnel sensors," *Appl. Phys. Lett.*, vol. 91, p. 102504-3, 2007.

[48] J. Scola, H. Polovy, C. Fermon, M. Pannetier-Lecoeur, G. Feng, K. Fahy, and J. M. D. Coey, "Noise in MgO barrier magnetic tunnel junctions with CoFeB electrodes: Influence of annealing temperature," *Appl. Phys. Lett.*, vol. 90, pp. 252501–252503, 2007.

[49] R. Stearrett, W. G. Wang, L. R. Shah, A. Gokce, J. Q. Xiao, and E. R. Nowak, "Evolution of barrier-resistance noise in CoFeB/MgO/CoFeB tunnel junctions during annealing," *J. Appl. Phys.*, vol. 107, pp. 064502–064507, 2010.

[50] F. G. Aliev, R. Guerrero, D. Herranz, R. Villar, F. Greullet, C. Tiusan, and M. Hehn, "Very low 1/f noise at room temperature in fully epitaxial Fe/MgO/Fe magnetic tunnel junctions," *Appl. Phys. Lett.*, vol. 91, p. 232504-3, 2007.

[51] H. Polovy, R. Guerrero, J. Scola, M. Pannetier-Lecoeur, C. Fermon, G. Feng, K. Fahy, S. Cardoso, J. Almeida, and P. P. Freitas, "Noise of MgO-based magnetic tunnel junctions," *J. Magn. Magn. Mater.*, vol. 322, p. 1624, 2009.

[52] C. Ren, X. Liu, B. D. Schrag, and G. Xiao, "Low-frequency magnetic noise in magnetic tunnel junctions," *Phys. Rev. B*, vol. 69, p. 104405, 2004.

[53] S. H. Liou, R. Zhang, S. E. Russek, L. Yuan, S. T. Halloran, and D. P. Pappas, "Dependence of noise in magnetic tunnel junction sensors on annealing field and temperature," *J. Appl. Phys.*, vol. 103, pp. 07E920–07E923, 2008.

[54] H. T. Hardner, M. J. Hurben, and N. Tabat, "Noise and magnetic domain fluctuations in spin-valve GMR heads," *IEEE Trans. Magn.*, vol. 35, pp. 2592–2594, 1999.

[55] K. Kandiah and F. B. Whiting, "Low frequency noise in junction field effect transistors," *Solid-State Electron.*, vol. 21, pp. 1079–1088, 1978.

[56] G. C. Han, B. Y. Zong, P. Luo, and C. C. Wang, "Magnetic field dependence of low frequency noise in tunnel magnetoresistance heads," *J. Appl. Phys.*, vol. 107, p. 09C706-3, 2010.

[57] Z. Jian-Gang and Z. Xiaochun, "Spin transfer induced noise in CPP read heads," *IEEE Trans. Magn.*, vol. 40, pp. 182–188, 2004.

[58] H. Xi, J. Loven, R. Netzer, J. I. Guzman, S. Franzen, and S. Mao, "Thermal fluctuation of magnetization and random telegraph noise in magnetoresistive nanostructures," *J. Phys. D: Appl. Phys.*, vol. 39, p. 2024, 2006.

[59] R. Landauer, "Solid-state shot noise," *Phys. Rev. B*, vol. 47, p. 16427, 1993.

[60] G. Lecoy and L. Gouskov, "Noise in thin films metal-oxide-metal $\mathrm{Al-Al_2O_3-Al}$," *Phys. Status Solidi B*, vol. 30, pp. 9–17, 1968.

[61] R. Kubo, "The fluctuation-dissipation theorem," *Rep. Prog. Phys.*, vol. 29, p. 255, 1966.

[62] A. Ozbay, A. Gokce, T. Flanagan, R. A. Stearrett, E. R. Nowak, and C. Nordman, "Low frequency magnetoresistive noise in spin-valve structures," *Appl. Phys. Lett.*, vol. 94, p. 202506-3, 2009.

[63] P. W. T. Pong, R. McMichael, A. S. Edelstein, E. R. Nowak, and J. W. F. Egelhoff, "Preliminary design and noise considerations for an ultrasensitive magnetic field sensor," *Proc. SPIE*, vol. 6645,, p. 66450T-12, 2007.

[64] X. Liu, C. Ren, and G. Xiao, "Magnetic tunnel junction field sensors with hard-axis bias field," *J. Appl. Phys.*, vol. 92, pp. 4722–4725, 2002.

[65] D. Mazumdar, X. Liu, B. D. Schrag, M. Carter, W. Shen, and G. Xiao, "Low frequency noise in highly sensitive magnetic tunnel junctions with (001) MgO tunnel barrier," *Appl. Phys. Lett.*, vol. 91, p. 033507-3, 2007.

[66] F. Guo, G. McKusky, and E. D. Dahlberg, "An investigation of the magnetic state dependent low frequency noise in magnetic tunnel junctions," *Appl. Phys. Lett.*, vol. 95, pp. 062512–062513, 2009.

[67] N. A. Stutzke, S. E. Russek, D. P. Pappas, and M. Tondra, "Low-frequency noise measurements on commercial magnetoresistive magnetic field sensors," *J. Appl. Phys.*, vol. 97, p. 10Q107-3, 2005.

[68] J. Cao and P. P. Freitas, "Wheatstone bridge sensor composed of linear MgO magnetic tunnel junctions," *J. Appl. Phys.*, vol. 107, pp. 09E712–09E713, 2010.

[69] H. H. Scholefield, R. V. Major, B. Gibson, and A. P. Martin, "Factors influencing the initial permeability of some alloys based on 80Ni20Fe," *British J. Appl. Phys.*, vol. 18, p. 41, 1967.

[70] P. Wisniowski, J. M. Almeida, and P. P. Freitas, "1/f magnetic noise dependence on free layer thickness in hysteresis free MgO magnetic tunnel junctions," *IEEE Trans. Magn.*, vol. 44, pp. 2551–2553, 2008.

[71] J. M. Almeida and P. P. Freitas, "Field detection in MgO magnetic tunnel junctions with superparamagnetic free layer and magnetic flux concentrators," *J. Appl. Phys.*, vol. 105, pp. 07E722–07E723, 2009.

[72] W. Shen, B. D. Schrag, A. Girdhar, M. J. Carter, H. Sang, and G. Xiao, "Effects of superparamagnetism in MgO based magnetic tunnel junctions," *Phys. Rev. B*, vol. 79, p. 014418, 2009.

[73] M. Tondra, J. M. Daughton, D. Wang, R. S. Beech, A. Fink, and J. A. Taylor, "Picotesla field sensor design using spin-dependent tunneling devices," *J. Appl. Phys.*, vol. 83, pp. 6688–6690, 1998.

[74] R. Guerrero, M. Pannetier-Lecoeur, C. Fermon, S. Cardoso, R. Ferreira, and P. P. Freitas, "Low frequency noise in arrays of magnetic tunnel junctions connected in series and parallel," *J. Appl. Phys.*, vol. 105, pp. 113922–113925, 2009.

[75] A. Jander, C. A. Nordman, A. V. Pohm, and J. M. Anderson, "Chopping techniques for low-frequency nanotesla spin-dependent tunneling field sensors," *J. Appl. Phys.*, vol. 93, pp. 8382–8384, 2003.

[76] A. S. Edelstein, G. A. Fischer, M. Pedersen, E. R. Nowak, S. F. Cheng, and C. A. Nordman, "Progress toward a thousandfold reduction in 1/f noise in magnetic sensors using an ac microelectromechanical system flux concentrator (invited)," *J. Appl. Phys.*, vol. 99, p. 08B317-6, 2006.

[77] A. Guedes, S. B. Patil, P. Wisniowski, V. Chu, J. P. Conde, and P. P. Freitas, "Hybrid magnetoresistive/microelectromechanical devices for static field modulation and sensor 1/f noise cancellation," *J. Appl. Phys.*, vol. 103, p. 07E924-3, 2008.

[78] J. E. Burnette, A. S. Edelstein, G. A. Fischer, E. Nowak, W. Bernard, S. F. Cheng, C. Nordman, and J. W. F. Egelhoff, "Initial studies on microelectromechanical system flux concentrators," *J. Appl. Phys.*, vol. 103, pp. 07E930–07E933, 2008.

[79] A. S. Edelstein, J. E. Burnette, G. A. Fischer, K. Olver, J. W. Egelhoff, E. Nowak, and S.-F. Cheng, "Validation of the microelectromechanical system flux concentrator concept for minimizing the effect of 1/f noise," *J. Appl. Phys.*, vol. 105, pp. 07E720–07E723, 2009.

[80] G. Jaramillo, C. Mei Lin, A. Guedes, and D. A. Horsley, "Fabrication of micromechanically-modulated MgO magnetic tunnel junction sensors," in *IEEE International Conference on Micro Electro Mechanical Systems (MEMS)*, 2010, pp. 667–670.

[81] R. C. L. Li, J. Unguris, A. S. Edelstein, J. E. Burnette, G. A. Fischer, E. R. Nowak, W. F. Egelhoff, and P. W. T. Pong, "Magnetic tunnel junction magnetic field sensor design tool," in *IEEE Int. Nanoelectronics Conf. (INEC)*, 2010, pp. 1149–1150.